

## NOTES AND CORRESPONDENCE

## Directional Spreading of Short Wavelength Fetch-Limited Wind Waves

M. L. HERON\*

*Physics Department, James Cook University, Townsville, Australia 4811*

30 April 1985 and 4 August 1986

## ABSTRACT

Observations of the spreading of short-wavelength (5 m) wind waves have been made with a steerable HF ocean surface radar in the nearshore zone in a stable offshore airflow. The directional spreading lobe is significantly broader than that predicted from the model by Hasselmann et al. It appears that the spreading lobe is broader at high frequencies ( $f \approx 0.56$  Hz) than at lower frequencies ( $0.2 < f < 0.5$  Hz) for  $f/f_m$  ratios near unity in a fetch-limited wind wave spectrum which has a peak at frequency  $f_m$ .

## 1. Introduction

Fixed-frequency narrow-beam HF ocean radars have been shown to be capable of observing the relative wave heights of surface gravity waves in the two propagation directions determined by the radar beam (Barrick, 1972). This arises through first-order Bragg scatter of grazing-incidence radio waves, of wavelength  $\lambda_0$ , from sea surface gravity waves of wavelength  $\lambda_0/2$  propagating along the same line which is radial with respect to the station. A Doppler shift separates the surface gravity wave propagating towards the radar station from the one propagating away. A typical 30 MHz groundwave radar spectrum is shown in Fig. 1 where peak B represents radar energy backscattered from the receding wave with 5 m wavelength, and peak A represents that for the approaching wave. In this case, since the receding waves have greater amplitude than the approaching waves, one can conclude that there is an acute angle between the radar beam and the wind vector.

Previous work has been done, using a single-lobe model for the wave directional spread, to estimate wind directions using observed ratios of the two first-order spectral energy density lines on radar backscatter spectra (Stewart and Barnum, 1975; Dexter and Casey, 1978; Maresca and Georges, 1980). The technique has been developed in these papers for synoptic scale windfield mapping over the oceans. Also the technique has been applied to mesoscale phenomena like sea-breeze cells in coastal waters (Dexter et al., 1985).

This technique makes some assumptions about the waveheight spectral density for sea surface gravity

waves. This spectral density is assumed to be of the form

$$E(f, \theta) = F(f)G(\theta). \quad (1)$$

The nondirectional spectral density term  $F(f)$  has been modeled by Hasselmann et al. (1973) and Hasselmann et al. (1976) in the form known as the JONSWAP spectrum. The technique for obtaining wind directions is not sensitive to the form of  $F(f)$  as long as the separation of variables in Eq. (1) holds. The  $G(\theta)$  term is usually assumed to be of the form

$$G(\theta) = A \cos^{2S}(\theta/2) \quad (2)$$

where  $\theta$  is the angle measured from the wind direction. Although this form is empirical it has found widespread usage both in wave buoy analysis (e.g., Longuet-Higgins et al., 1963; Mitsuyasu et al., 1975; Hasselmann et al., 1980) and in HF radar analysis.

An unfortunate notation difference has occurred whereby Longuet-Higgins et al. (1963) use  $\cos^S(\theta/2)$  for the waveheight distribution but Tyler et al. (1974) use  $\cos^S(\theta/2)$  for the variance distribution. Subsequent literature confuses the factor of 2. A plea is made for uniformity and it is suggested that Eqs. (1) and (2) be adopted by the HF radar community.

Several experiments have been done comparing HF radar derived wind directions with direct in situ observations. Stewart and Barnum (1975) used an algorithm for  $S$  that depended upon wind speed and radar wavelength. They showed that this was an improvement over a method used by Long and Trizna (1973) which did not include those parameters. Stewart and Barnum (1975), Dexter and Casey (1978), Heron et al. (1985) all use a form for  $S$  which is based on the work of Tyler et al. (1974) in which drag coefficients (Wu, 1969) were used to derive a parameter  $\mu$  such that

\* Work done while on leave at Centre for Water Research, University of Western Australia.

$$\mu = 3.65 \times 10^{-6} U^{5/4} f_0^{1/2}, \quad U \leq 15 \text{ m s}^{-1}$$

$$\mu = 8.33 \times 10^{-6} U f_0^{1/2}, \quad U \geq 15 \text{ m s}^{-1} \quad (3)$$

and then

$$S = 0.2(\mu - 0.1)^{-1}, \quad \mu \geq 0.2$$

$$S = 2, \quad \mu \leq 0.2. \quad (4)$$

Note that for all cases  $S \leq 2$ . This model has been fairly well tested in determining wind directions under a range of wind speeds and radar frequencies between 2 and 30 MHz.

The aim of this paper is to observe the wave-spreading lobe using a steerable narrow beam 30 MHz radar in fetch limited conditions to derive  $S$  values. These  $S$  values are compared with values obtained from a fetch-limited wave generation model described by Hasselmann et al. (1973) and Hasselmann et al. (1980). The motivation for this study is to evaluate the applicability of the model to the estimation of  $S$  values routinely in algorithms for producing wind directions from HF radar observations.

## 2. Model

Kitaigorodskii's (1962) suggestion to scale wave parameters according to the nondimensional fetch can be applied by using

$$\xi = gx/U^2 \cos \phi \quad (5)$$

where  $x$  is the distance offshore and  $\phi$  is the acute angle between the wind vector and the normal to the straight shoreline. In modeling for  $S$ , Hasselmann et al. (1980) suggest

$$S = S_m (f/f_m)^\mu, \quad f > f_m \quad (6)$$

where

$$S_m = 9.77 \pm 0.43 \quad (7)$$

$$\mu = -(2.33 \pm 0.06) - (1.45 \pm 0.45)(U/c_m - 1.17) \quad (8)$$

and the subscript  $m$  refers to values at the maximum wave amplitude in the wind-wave spectrum. Hasselmann et al. (1973) found that  $f_m$  depends on fetch according to

$$f_m = (g/U) 3.5 \xi^{-0.33} \quad \xi \leq 17\,000 \quad (9)$$

so that as the fetch  $\xi$  increases  $f_m$  becomes less. For  $\xi \geq 17\,000$  the fully developed spectrum given by Pierson and Moskowitz (1964) has<sup>1</sup>

$$f_m = 0.14g/U. \quad (10)$$

<sup>1</sup> The constant 0.14 applies to winds at 19.5 m altitude but has been used with 10 m winds (e.g., Hasselmann et al., 1976; Hasselmann et al., 1973). The value of the constant is not critical here.

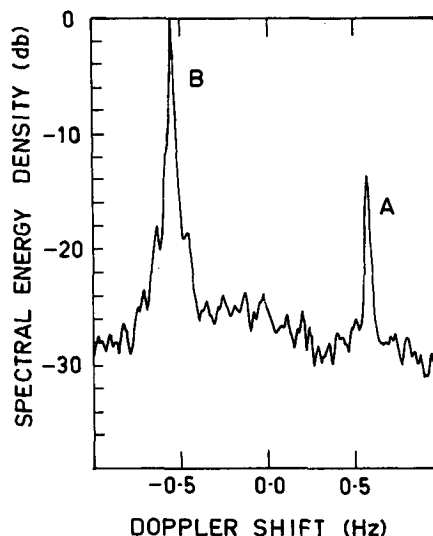


FIG. 1. A typical energy density spectrum for the HF ocean radar. Peaks A and B are the first-order Bragg-scatter lines which represent energy scattered from  $\lambda = 5$  m waves propagating towards A and away from B the radar site respectively.

On putting  $C_m = g/2\pi f_m$  for the wave celerity at the peak, the exponent in Eq. (6) is

$$\mu = -2.33 - 1.45(21.99\xi^{-0.33} - 1.17). \quad (11)$$

The 30 MHz HF radar used for the present work has a primary response to sea surface waves having wavelength 5 m. This corresponds to a wave frequency of 0.56 Hz, which is above the normal frequency range for directional wave buoy data. The radar is used to estimate the parameter  $S$ , in Eq. (2), for the width of the directional spreading lobe for the 5 m waves. The observations are made under fetch-limited conditions of wind speed and action distance.

The motivation for this experiment arises from the absence of high values for  $S$  ( $\geq 2$ ) in preliminary results. This suggests a significant departure from Eq. (6), especially if  $f_m$  is close to 0.56 Hz. The experimental parameters were chosen so that despite inherent uncertainties in environmental conditions and models, we could be reasonably sure that the condition  $f_m = 0.56$  Hz existed within our range.

## 3. Observational network

Our HF coastal ocean surface radar operates at a fixed frequency of 30 MHz and transmits and receives into a narrow beam which has effective radar width of  $3.5^\circ$ . The beam is steerable. Spectra like that in Fig. 1 are produced for all 3 km length range cells in a given sector in 102.4 seconds (Fig. 2).

The deployment was at Fremantle in Western Australia as shown in Fig. 2. The time was chosen on advice from the Australian Bureau of Meteorology to coincide

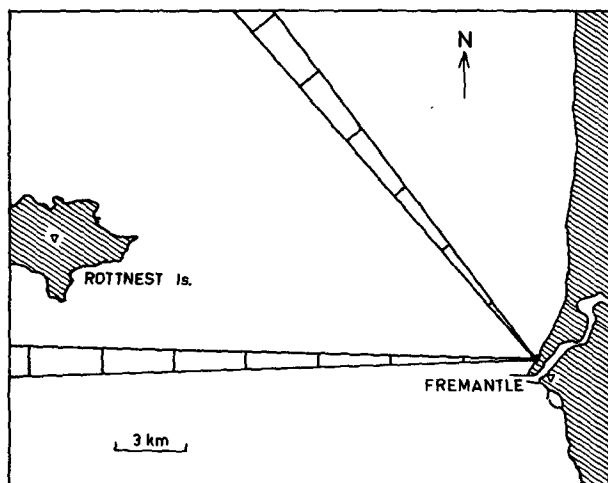


FIG. 2. The experiment site showing the two selected beam azimuths. The assumption is made that the wind and wave fields are independent of longshore displacement and functions of offshore dimension. Fremantle is located at  $31^{\circ}03'S$ ,  $115^{\circ}44'E$ .

with an easterly (offshore) gradient wind. Two beam positions were chosen at  $269.4^{\circ}E$  and  $321.4^{\circ}E$  as shown in Fig. 2. This allows the evaluation of two free parameters: the wind direction, which is assumed to be the direction of the lobe of wind-wave spread, and the spreading parameter  $S$ , which governs the width of the wind-wave lobe.

For a given beam direction the spectral density peaks A, B, (Fig. 1) have a ratio  $R$  derived from equation 2 to be

$$R = \left| \cos^{2S} \left( \frac{\theta + \pi}{2} \right) / \cos^{2S} \left( \frac{\theta}{2} \right) \right|$$

giving

$$\theta = |2 \arctan(R^{1/2S})|$$

where  $\theta$  is the direction of the lobe maximum measured from the beam position.

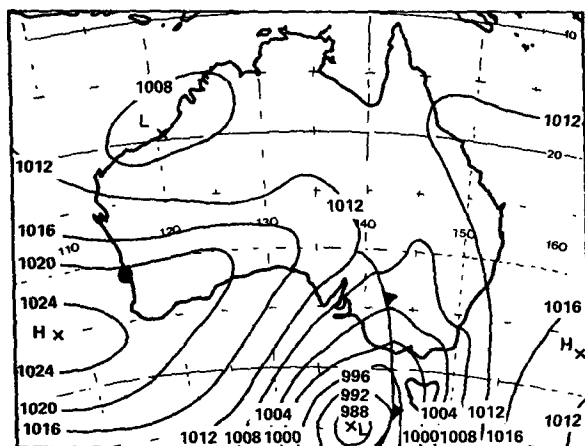
Data were available from two recording anemometers near the radar site and a remote station on Rottneest Island (21 km offshore) gave a ten minute average on request. Synoptic charts and onshore radiosonde data were available from the Bureau of Meteorology.

#### 4. Results

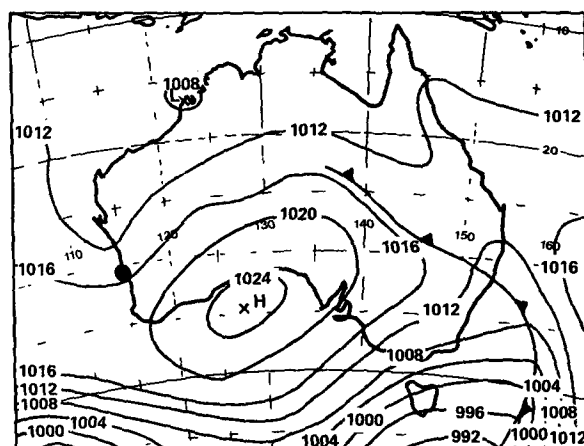
The synoptic ground-level pressure maps at 1000 LST (Western Australian Standard Time, WAST) 13 and 14 March (Fig. 3) indicate a slowly backing gradient wind due to a large scale intrusion of low pressure from the north.

Observed wind speeds and directions are shown on Fig. 4 for the 22 hour period around the radar operation time. Before noon on 14 March 1984 the wind source direction is northeast backing to north. The beach station is sheltered from easterlies by sand dunes, so those low windspeeds are false. The wind at Rottneest Island is offset about  $20^{\circ}$  to the east over the whole morning, but there is no variation in wind speed with distance offshore. A strong temperature inversion showing on the regular 0700 LST radiosonde release on 14 March 84 may have caused a catabatic wind component during the night. This would be an easterly component due to a north-south escarpment about 40 km inland. The large disturbance to the wind field after noon is a sea breeze change. The period before noon is available for the fetch-limited wind-wave generation experiment.

Two periods were chosen, i.e., when the offshore wind was reasonably constant, for radar data analysis. In the first period (0130–0300 LST) 14 pairs of  $\theta$ ,  $S$  values were calculated at each distance offshore and in the second period (1000–1230) hours 19 pairs were obtained at each distance. Thus a total of 118  $\theta$ ,  $S$  pairs



10am 13th MARCH 1984



10am 14th MARCH 1984

FIG. 3. Surface synoptic maps at 1000 LST 13 and 14 March 1984 (from Mon. Wea. Rev.). The experiment site is shown (●) on the West Australian coast.

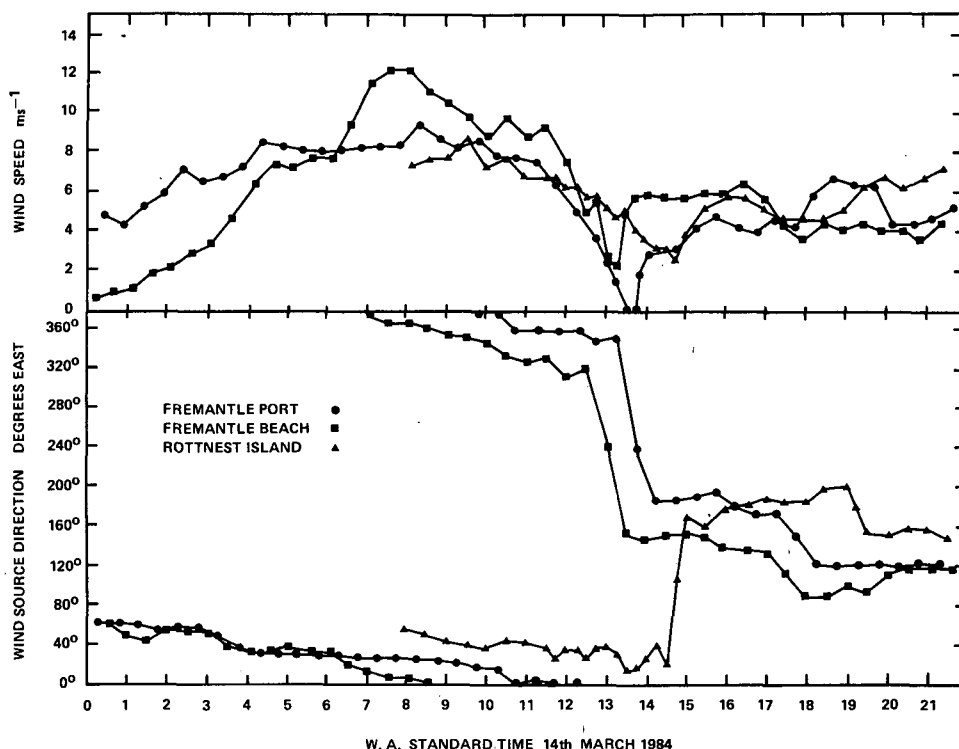


FIG. 4. Wind speed and direction observed at the Fremantle beach, Fremantle Port and Rottnest Island. The beach site is sheltered from easterlies, the Port site is  $\sim 60$  m AGL and the island site is 21 km offshore. Three regimes: before 1300, between 1300 and 1500, and after 1500 LST are identified for separate analysis of radar data.

are represented on Fig. 5. The error estimate on the means is indicated on Fig. 5.

## 5. Discussion

Figure 5 shows that all the mean  $S$  values observed during the experiment are less than 1.6. During the experiment the wind was offshore, with calm water near the coast and ideal wind-wave generation conditions occurring in the radar beam. The fetches involved in our experiment are short and we need to carefully examine the limits on the validity of the empirical wave generation Eqs. (6) and (9). That is to examine the extent of the data base from which they were derived.

Equation (9), given by Hasselmann et al. (1973), is derived empirically from data in the approximate ranges  $0.2 \leq f_m U/g \leq 10$  and  $0.1 \leq \xi \leq 10^4$ . Within the dataset, ranges  $50 \leq \xi \leq 10^4$  and  $0.2 \leq f_m U/g \leq 1.0$  were taken from the sea and the rest from laboratory tanks. Conditions for the offshore end of our transect are shown in Table 1 and it is clear that Eq. (9) is valid there. The wind-wave spectrum was developing from calm onshore to  $f_m \approx 0.35$  Hz at the maximum range. Somewhere within that range the condition  $f/f_m = 1$  (for  $f = 0.56$  Hz) is assumed to be satisfied. But over our entire range  $s \leq 1.6$  is observed. This has implications for Eq. (6).

Equation (6), given by Hasselmann et al. (1980), is derived empirically from data in the approximate ranges  $0.14 \leq f_m \leq 0.24$  Hz and  $1.0 \leq U/C_m \leq 1.78$ . Also the maximum wave frequency observed for the database was  $f = 0.5$  Hz. Table 1 shows that the conditions of Eq. (6) are not satisfied at our extreme range. And the departure is even greater at shorter fetches.

The conclusion is that Eq. (6) does not hold for  $f = 0.56$  Hz when  $f/f_m \approx 1$ . Note that these values lie outside the database on which the existing empirical Eq. (6) is based. The results apply to processes outside the range of the empirical model and therefore they extend that model and do not destroy it. In the early states of development, when  $f_m \approx 0.56$  Hz the directional spreading of the waves is very broad.

Figure 5 is drawn on an abscissa which uses Eq. (9) to illustrate the difference between  $S$  values observed and predicted. This experiment does not investigate the relationship between  $f_m$  and  $\xi$  (Eq. (9)) so the abscissa in Fig. 5 is scaled assuming that Eq. (9) applies to sea waves at frequencies near 0.56 Hz. The highest  $f/f_m$  points are close to the validated range for Eq. (9) in sea conditions.

The data points are mean  $S$  values at each  $f/f_m$  available. Also on Fig. 5 is shown the regression line drawn by Hasselmann et al. (1980) through their wave-buoy data; the broken lines are one standard deviation from

the regression. The confidence that the radar data points lie below the wave-buoy regression on Fig. 5 is greater than 99.99%.

The wave-buoy data in Hasselmann et al. (1980) were taken in the range  $0.14 \leq f_m \leq 0.25$  Hz while the observed wind waves were in the frequency range  $0.07 < f < 0.5$  Hz. The radar data were limited to  $0.36 < f_m < 0.56$  Hz. This happens because we are limited to observing only the waves with 5 m wavelength ( $f = 0.56$  Hz) and we rely on radar range (fetch) to give variations in  $f_m$ . Therefore, while the parameterization of Eq. (9) may allow us to represent both data sets in the same form (Fig. 5), it is pointed out that they represent different wave conditions. In particular the range of  $f_m$  for the radar data represents very short fetch conditions.

## 6. Conclusion

This is a limited study which does not cover a wide range of wind-wave generation conditions. The assumptions made here are the ones normally made in each of the two branches of wind-wave techniques which we are comparing. The result that the observed  $S$  values fall significantly below the model values near  $f/f_m \approx 1$  suggests that the empirical model [Eq. (6)] does not extend to  $f \approx 0.56$  Hz.

The result that  $S$  does not go through a high excursion near  $f/f_m \approx 1$  for short wind-waves is significant for people using HF radar for wind direction observations. The empirical limit  $S \leq 2$  imposed by Tyler et al. (1974) is supported for short wind waves in fetch limited regimes.

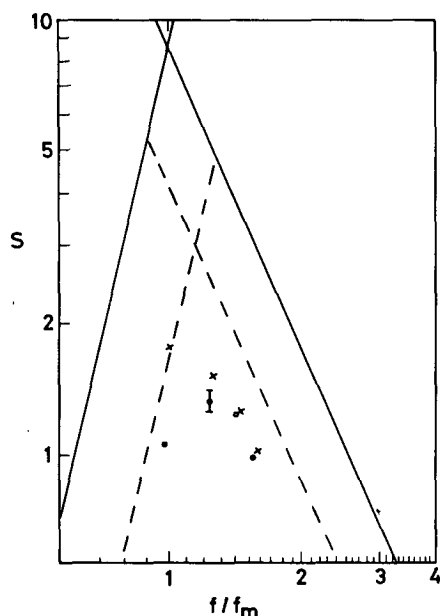


FIG. 5.  $S$  values for  $U = 8.5 \text{ m s}^{-1}$  ( $\times$ ) and  $U = 6.5 \text{ m s}^{-1}$  ( $\circ$ ) from HF ocean radar data where  $f = 0.56$  Hz. The solid line is the regression on wave buoy data  $0.26 < f < 0.5$  Hz by Hasselmann et al. (1980). The broken line indicates the standard deviation from the regression.

TABLE 1. Wave generation conditions at the offshore extremity of the observation range.

$U = 8.5 \text{ m s}^{-1}$	$U = 6.5 \text{ m s}^{-1}$	Comment
$\phi = 0^\circ$	$\phi = 36^\circ$	Equation 5
$x = 12000 \text{ m}$	$x = 12000 \text{ m}$	Equation 5
$\xi = 1628$	$\xi = 3441$	Equation 5
$f_m = 0.35 \text{ Hz}$	$f_m = 0.36 \text{ Hz}$	Equation 9
$f_m = 0.30$	$f_m = 0.24$	$f_m = f_m U/g$
$U/C_m = 1.91$	$U/C_m = 1.50$	$C_m = g/2\pi f_m$

**Acknowledgments.** The Coastal Ocean Surface Radar (COSRAD) facility was instigated under Australian Research Grants Scheme funding and this project was funded by the Australian Marine Sciences and Technologies Scheme. We appreciate the assistance from the Bureau of Meteorology and the Fremantle Port Authority.

## REFERENCES

- Barrick, D. E., 1972: First order theory and analysis of MF/HF/VHF scatter from the sea. *IEEE Trans. Antenna Propag.*, **AP-20**, 2-10.
- Dexter, P. E., and R. Casey, 1978: Ocean windfield mapping at long ranges with an HF radar. *Aust. Meteor. Mag.*, **26**, 33-44.
- , M. L. Heron and B. T. McGann, 1985: A tropical winter sea-breeze observed with an HF groundwave radar. *Aust. Meteor. Mag.*, **33**, 117-128.
- Hasselmann, D. E., M. Duncel and J. A. Ewing, 1980: Directional wave spectra observed during JONSWAP 1973. *J. Phys. Oceanogr.*, **10**, 1264-1280.
- Hasselmann, K., T. P. Barnett, E. Bouws, H. Carlson, D. E. Cartwright, K. Enke, J. A. Ewing, H. Gienapp, D. E. Hasselmann, P. Kruseman, A. Meerburg, P. Muller, D. J. Olbers, K. Richter, W. Sell and H. Walden, 1973: Measurements of windwave growth and swell decay during the Joint North Sea Wave Project (JONSWAP). *Dtsch. Hydrogr. Z.*, **A8**(Suppl.), 12, 93 pp.
- , D. B. Ross, P. Muller and W. Sell, 1976: A parametric wave prediction model. *J. Phys. Oceanogr.*, **6**, 200-228.
- Heron, M. L., P. E. Dexter and B. T. McGann, 1985: Parameters of the air-sea interface by HF ground-wave Doppler radar. *Aust. J. Freshwater Mar. Sci.*, **36**, 655-70.
- Kitaigorodskii, S. A., 1962: Applications of the theory of similarity to the analysis of wind-generated wave motion as a stochastic process. *Bull. Acad. Sci. USSR Geophys.*, Ser. No. 1, 73.
- Long, A. E., and D. B. Trizna, 1973: Mapping of North Atlantic winds by HF radar sea backscatter interpretation. *IEEE Trans. Antennas Propag.*, **AP-21**, 680-685.
- Longuet-Higgins, M. S., D. E. Cartwright and N. D. Smith, 1963: Observations of the directional spectrum of sea waves using the motions of a floating buoy. *Ocean Wave Spectra*. Prentice Hall.
- Maresca, J. W., Jr., and T. M. Georges, 1980: Measuring rms wave height and the scalar ocean wave spectrum with HF skywave radar. *J. Geophys. Res.*, **85**, 2759-2771.
- Mitsuyasu, H., F. Tasai, T. Suhara, S. Mizuno, M. Ohkusu, T. Honda and K. Rikiishi, 1975: Observations of the directional spectrum of ocean waves using a cloverleaf buoy. *J. Phys. Oceanogr.*, **5**, 750-760.
- Pierson, W. J., and L. Moskowitz, 1964: A proposed spectral form for fully developed wind seas based on the similarity theory of S. A. Kitaigorodskii. *J. Geophys. Res.*, **69**, 5191-5203.
- Stewart, R. H., and J. R. Barnum, 1975: Radio measurements of oceanic winds at long ranges: An evaluation. *Radio Sci.*, **10**, 853-857.
- Tyler, G. L., C. C. Teague, R. H. Stewart, A. M. Munk and J. W. Joy, 1974: Wave directional spectra from synthetic aperture observations of radio scatter. *Deep-Sea Res.*, **21**, 989-1016.
- Wu, J., 1969: Wind stress and surface roughness at air-sea interface. *J. Geophys. Res.*, **74**, 444-455.
- Reference is also made to the "Monthly Weather Review, Western Australia" Bureau of Meteorology, Perth, March, 1984.